Systematic Analysis on the Optical Properties of Chiral Metamaterial Slab for Microwave Polarization Control

I. Comez [1], M. Karaaslan [2], F. Dincer [3], F. Karadag [1], and C. Sabah [4]

[1] Department of Physics
Cukurova University, Adana, Turkey

[2] Department of Electrical and Electronics Engineering
[3] Department of Computer Engineering
Mustafa Kemal University, Iskenderun, Hatay, Turkey

[4] Department of Electrical and Electronics Engineering
Middle East Technical University ─ Northern Cyprus Campus
Kalkanli, Guzelyurt, TRNC/Mersin 10, Turkey
sabah@metu.edu.tr

Abstract ─ Theoretical and numerical of investigation of the chiral slab exhibiting polarization rotation is presented in detail. The effects of the chirality, thickness of medium, dielectric constant, and incident angle are analyzed in order to display the characteristic features of the chiral slab both for TE and TM incident waves. The chiral slab then is realized by using a full wave EM simulation software in order to validate the numerical results in which the numerical and simulation results are in good agreement with each other. Different than the other studies existing in literature, the proposed model shows optimum results for wide frequency band by using small chirality which is sufficient for polarization rotation. From the results, it is observed that the proposed system and its realization can be effectively used as a polarization converter and EM filters at some frequencies.

Index Terms ─ Chirality, EM filter metamaterial, polarization control.

I. INTRODUCTION

Chiral medium has received considerable attention in last decades due to their potential applications (such as filters, polarization rotators, antennas, and so on) in microwave and millimeter wave frequencies [1-5]. It can be realized using several methods [6-9] including metamaterials (MTMs) without mirror symmetry planes [10] to exhibit, for some desired aims, a controlled active, dynamical, and tunable EM response [11]. Chiral medium is characterized by the quantity of chirality, $\xi = (n_R - n_L)/2$, where n_R and n_L is the refractive index of the right- and left-handed circular polarized wave (RCP and LCP) [12,13]. Basically, chirality is defined as the lack of mirror image symmetry which refers to the ability of the polarization rotation. In this sense, it is always desirable to have full control of the polarization states of EM waves especially for filtering, data transmission, and sensing purposes. The polarization control can effectively be manipulated through the reflection/refraction using a chiral slab (CS) or chiral MTM (CMTM) owing to the strong polarization rotation ability due to lack of mirror symmetry. This is also known as optical activity and can be used in many fields as polarizers, diagnostic tool in spectroscopy and analytical chemistry, signature effect for the life detection in molecular biology [14-22]. Besides, oriented or randomly arranged man made metal helices was investigated as polarizer which exhibits large circular dichroism and huge polarization rotation as in the new-generation MTMs [21], [22]. Additionally, the reflection and transmission properties of multiple chiral layers are analyzed to

Submitted On: January 14, 2014
Accepted On: March 29, 2015

show the polarization conversion and EM filtering features of the conventional CSs [8], [9].

In this work, methodical investigation of a CS and its characteristic features are studied. First, the electromagnetic properties of the chiral medium are given. Then, theoretical equations for the CS are established. After that, the numerical analysis based on the theoretical formalism are provided by considering the effects of the different parameters such as chirality coefficients, thickness of medium, dielectric constant, and incident angle. Reflection and transmission coefficients through the CS are computed and presented for the incident wave of TE and TM cases. From the results, it can be seen that CS can be used as a polarization-convertor and EM filter (transmission and/or antireflection) at around the operation/central frequency. As a final investigation, the studied CS are constructed physically by a simulation software to be able to validate the numerical results and to show the feasibility of the proposed system. The constructed CS by the simulation software shows very good performance and can be fabricated for the experimental study to be used as EM filter or polarization-rotator [8], [9]. Commonly, these kinds of devices are generally realized using more than one-slab [4], [5], [8], [9]. However, the realization is accomplished using *only-one-slab* in the present study. Additionally, the new generation CMTMs have very large chirality values which creates some difficulties in the design and realization of mentioned devices. Keeping the chirality values small enough abolish the difficulties and makes the EM filter and polarization-rotator devices easily realizable. Those are main advantages of the present study and provide additional flexibilities to design and manufacturing processes.

II. THEORETICAL ANALYSIS

CS has interesting properties when it is embedded between two semi-infinite dielectrics. The configuration of the structure is shown in Fig. 1. TE and TM polarized monochromatic plane incident wave from free-space is applied to CS. In general, wave equation in a chiral media can be given as [8], [23]:

$$\vec{\nabla}\times\vec{\nabla}\times\vec{\varphi}-2\omega\mu\xi\vec{\nabla}\times\vec{\varphi}-k^2\vec{\varphi}=0, \quad (1)$$

where ξ is the chirality of CS; k is the wave number, and $\vec{\varphi}$ is the field. If the field $\vec{\varphi}$ is along p direction and the field have two components along q and r orthogonal directions, it can be written as:

$$\vec{\varphi}=(q\overrightarrow{a_q}+r\overrightarrow{a_r})e^{kp}. \quad (2)$$

The left (LCP) and right (RCP) circularly polarized components of propagation $k_{LCP,\ RCP}$ are determined using of Eqs. (1) and (2) as [8], [23]:

$$k=-jk_{LCP,\ RCP}=-j\left[\omega\mu\xi\pm\sqrt{\omega^2\mu\hat{I}+(\omega\mu\xi)^2}\right]. \quad (3)$$

The relation between incidence, transmission and reflection angles is obtained by Snells Law [8], [23]:

$$k_i\sin\theta_i=k_R\sin\theta_R=k_L\sin\theta_L=k_t\sin\theta_t\,;\theta_i=\theta_r, \quad (4)$$

where θ_i is the incidence angle, θ_r is the reflection angle; and θ_R and θ_L are the angles of right and left polarized components of the transmitted wave. The incident, reflected, and transmitted with respect to Fig. 1 can be determined as follows.

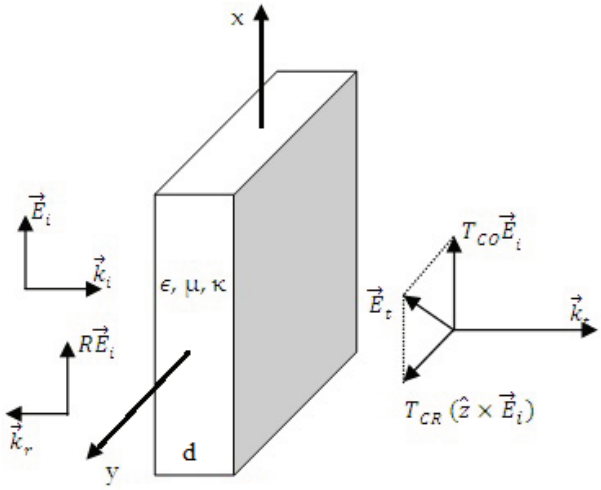

Fig. 1. Schematic diagram of CS with incident, reflected, and transmitted fields

According to Fig. 1, the incident electric field with arbitrary polarization composed of TE and TM components can be written as [8], [23]:

$$\boldsymbol{E}_i=(E_0^{TM}.\boldsymbol{u_{TM}}+E_0^{TE}.\boldsymbol{u_{TE}})e^{-jk_tr}.e^{-j\gamma p}, \quad (5)$$

where E_0^{TM} and E_0^{TE} are the components of incident electric field; $\boldsymbol{u_{TE}}$ and $\boldsymbol{u_{TM}}$ denotes direction vectors of TE and TM electric field components, and k_t represents the transverse component of wave vector. TE and TM refer to the parallel and perpendicular components of the electric field vector. Note that, the first region is selected as

vacuum. Then, the reflected electric ($\boldsymbol{E}_r$) field can be written as [8], [23]:

$$\boldsymbol{E}_r = (E_r^{TM}\boldsymbol{u_{TM}} + je_r^{TE}\boldsymbol{u_{TE}})e^{-jk_T r}e^{j\gamma p} + (E_r^{TE}\boldsymbol{u_{TE}} + je_r^{TM}\boldsymbol{u_{TM}})e^{-jk_T r}.e^{j\gamma p}, \quad (6)$$

where e_r^{TM} and $e_r^{TE}$are the components of the reflected electric field. The electric field is represented with RCP and LCP components in Eq. (6). As a next step, the fields in CS will be given. The electric field in CS has also two components (RCP and LCP) and they are propagating both in positive and negative directions. Therefore, in CS there are two waves, one propagating along the same direction with the incident wave and the other one propagating toward the opposite of the incident wave. Thus, the total electric field in CS can be expressed as [8], [23]:

$$\boldsymbol{E}^+ = (A_L^{TM}\boldsymbol{u_{TM}} + jA_L^{TE}\boldsymbol{u_{TE}})e^{-jk_T r}e^{-j\gamma_L p} + (A_R^{TM}\boldsymbol{u_{TM}} - jA_R^{TE}\boldsymbol{u_{TE}})e^{-jk_T r}e^{-j\gamma_R p} + (jA_L^{TM}\boldsymbol{u_{TM}} - jA_L^{TE}\boldsymbol{u_{TE}})e^{-jk_T r}e^{-j\gamma_L p} + (jA_R^{TM}\boldsymbol{u_{TM}} + A_R^{TE}\boldsymbol{u_{TE}})e^{-jk_T r}e^{-j\gamma_R p}, \quad (7.a)$$

$$\boldsymbol{E}^- = (B_L^{TM}\boldsymbol{u_{TM}} - jB_L^{TE}\boldsymbol{u_{TE}})e^{-jk_T r}e^{j\gamma_L p} + (B_R^{TM}\boldsymbol{u_{TM}} - jB_R^{TE}\boldsymbol{u_{TE}})e^{-jk_T r}e^{j\gamma_R p} + (-jB_L^{TM}\boldsymbol{u_{TM}} - B_L^{TE}\boldsymbol{u_{TE}})e^{-jk_T r}e^{j\gamma_L p} + (-jB_R^{TM}\boldsymbol{u_{TM}} - B_R^{TE}\boldsymbol{u_{TE}})e^{-jk_T r}e^{j\gamma_R p}, \quad (7.b)$$

where A_L^{TM},A_L^{TE},A_R^{TM},A_R^{TE} and B_L^{TM},B_L^{TE},B_R^{TM},B_R^{TE} are the amplitudes of the electric fields in CS. Note that, in all representations, the subscripts *L*, *R*, TM, and TE denotes the LCP, RCP, transverse electric, and transverse magnetic components of electric field, correspondingly. The electric fields in the last region can also be expressed in terms of both TE and TM components. Third region is also vacuum as in the first region. The transmitted electric field with any arbitrary polarization can be written as follows [8], [23]:

$$\boldsymbol{E_t} = (E_t^{TM}\boldsymbol{u_{TM}} + je_t^{TE}\boldsymbol{u_{TE}})e^{-jk_T p}e^{-j\gamma(z-d)} + (jE_t^{TM}\boldsymbol{u_{TM}} + e_t^{TE}\boldsymbol{u_{TE}})e^{jk_T p}e^{-j\gamma(z-d)}, \quad (8)$$

where E_t^{TM} and e_t^{TE} are TM and TE components of electric field and d is the thickness of CS. The corresponding magnetic fields for all regions can be found using Maxwell's equations [8], [23]. In order to analyze the proposed configuration, it is required to impose the boundary conditions at the interfaces of $z = 0$ and $z = d$. Therefore, the relationships between the fields in all regions can easily be determined by using the boundary conditions and Maxwell's equations. As a result, the reflection and transmission coefficients can be found and computed [8], [23].

III. NUMERICAL RESULTS

In this section, co- (TE-TE or TM-TM) and cross-polarized (TE-TM or TM-TE) reflection and transmission coefficients are presented numerically to observe their behaviors using the theory of the previous section. Particularly, the effects of the chirality, thickness of the slab, dielectric constant, and incident angle will be investigated and analyzed in details by means of the numerical computations. In order to verify the computations, a particular case is simulated using a commercial full-wave software. Both processes give the same results, which means the numerical computations are verified.

A. Effect of the chirality on the reflection and transmission

One of the main parameters that affect the polarization state of the wave and provides polarization conversion is the chirality. Here, the effects of the chirality parameter on the reflection and transmission will be investigated. The incident and transmitted media are defined as free space ($\mu_i = \mu_t = \mu_0,\ \varepsilon_i = \varepsilon_t = \varepsilon_0$) and CS has the following parameters: $\varepsilon_c = 4\varepsilon_0,\ \mu_c = \mu_0,\ d = 3\ mm$. Note that, the selected chirality values are so small that its influence on the refractive index is negligible. However, it is carefully selected and its absolute value has to be lower than the upper bound resulting from maximum coupling and given by $|\xi_c| \leq \sqrt{\varepsilon/\mu}$ where ε and μ are permittivity and permeability of the medium [6], [8], [24], [25]. The optimum value is chosen for this study to provide sufficient coupling between the electric and magnetic fields. Note those Refs. [6,24] emphasize that even a small value of ξ_c can have a pronounced effect on the transmitted wave through rotation of the polarization. Note again, for the selected optimum chirality value, there exists a symmetry in the reflection and transmission with respect to the resonant frequency but the symmetry can be lost for different chirality values [8]. Figure 2 shows the reflection and transmission response with respect to frequency when the chirality varied. The increase in the chirality shifts the resonant frequency downward due to the inverse proportionality between the frequency and chirality (Eq. 3). Quasi-

reflection band-pass phenomenon is observed for all polarizations when the chirality parameter is varied. Thus, semi-band-pass EM filter for the reflected wave can be utilized using the proposed configuration. More importantly, the structure provides a wide-band polarization conversion in the transmitted wave at the resonant frequency for all chirality parameters. For example, parallel to perpendicular (TM to TE) polarization conversion occurs for the transmitted wave for $\xi_c = 0.003$ at the resonant frequency of 22.1 GHz, although the incident electric field has no perpendicular component at all (optical activity and polarization rotation with 100 % efficiency). The same observation are also scrutinized for the perpendicular to parallel (TE to TM) polarization conversion at the mentioned resonant frequency, since CS is a symmetric structure with respect to its front and back sides. Note that, similar polarization conversion cases (with ~100% efficiency for all cases) can also be seen for the other chirality parameters. Consequently, the small chirality leads to a polarization-rotated transmitted wave. At the resonant frequency, almost complete parallel-to-perpendicular or perpendicular-to-parallel conversions occur for the transmitted wave. Therefore, one can say that the proposed structure acts as a wide-band polarization-conversion transmission filter and antireflection (full-transmission) in some microwave frequency band.

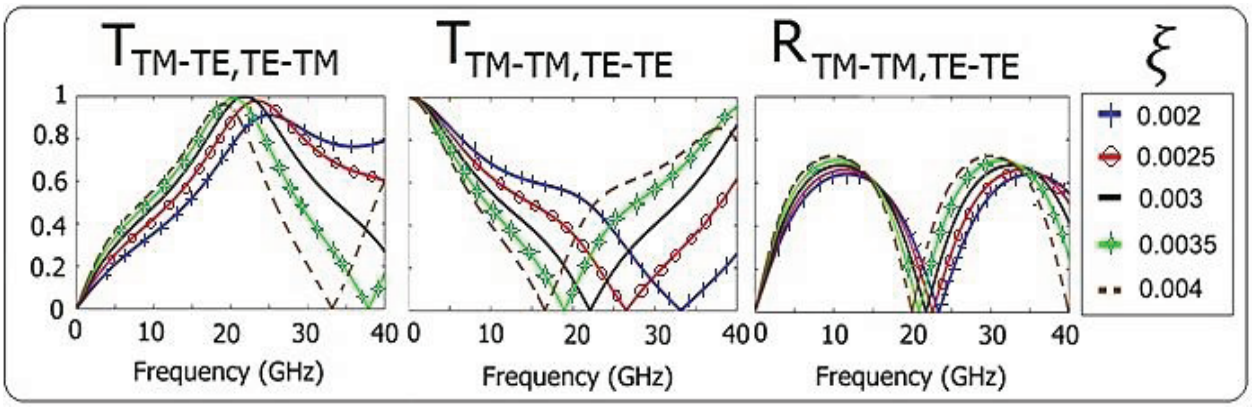

Fig. 2. Cross- and co-polarized transmission; and co-polarized reflection coefficients versus frequency with respect to the chirality variation.

B. Effect of the dielectric constant on the reflection and transmission

Another parameter that affect the reflection and transmission features of the system is the dielectric constant of CS. The incident and transmitted media are defined as free space. CS has the following parameters: $\mu_c = \mu_0$, $d = 3\,mm$ and $\xi_c = 0.003$. Figure 3 presents the reflection and transmission data. Quasi-reflection band-pass phenomenon (semi-bandpass EM filter property) for the reflected wave, as in the previous case, is also observed for both polarizations when the dielectric constant of CS is changed. The co-polarized (TE-TE or TM-TM) transmission is zero and the cross-polarized (TE-TM or TM-TE) transmission has a high peak (unity or close to unity) at the resonant frequency (~20 GHz) while the incident EM wave has no cross-polarized field component(s). It means that broad spacing of transmission peak is preserved and wide-band complete polarization conversion occurs at this frequency. Consequently, the proposed structure is insensitive to the variation of the dielectric constant of CS and this property can be regarded as an added value of the model which provides additional flexibility in the design, optimization, and fabrication processes.

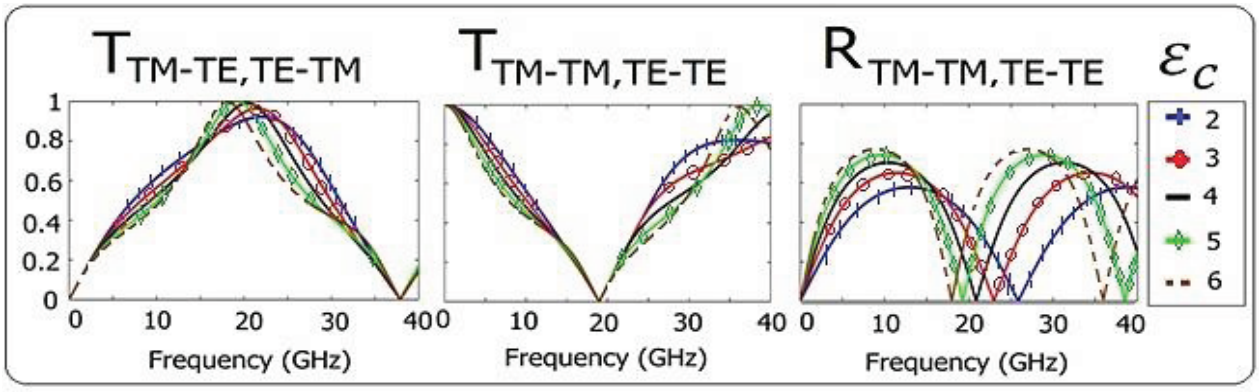

Fig. 3. Cross- and co-polarized transmission; and co-polarized reflection coefficients versus frequency with respect to the variation of the dielectric constant of CS.

C. Effect of the slab thickness on the reflection and transmission

In this section, the effect of the slab thickness on the character of the reflection and transmission will be analyzed. The incident and transmitted media are defined as free space as in the previous example. The CS has the following parameters: $\xi_c = 0.003$, $\mu_c = \mu_0$, and $\varepsilon_c = 4\varepsilon_0$. The results are shown in Fig. 4. Quasi-reflection band-pass for the reflected wave and polarization conversion for the transmitted wave occur (as in the previous two cases) regardless of the change in the thickness of CS. The increase in the thickness of CS yields a down-shift in the resonant frequency (and thus a down-shift in the cross-polarized transmission peak). Complete polarization conversion (with fully anti-reflection property) for the transmitted wave occurs at the resonant frequency for the selected medium parameters for different thicknesses. The spectral location of the resonance is inversely proportional with the thickness of CS. Consequently, the proposed structure is independent from the change of the thickness of CS. This means that more flexible prototype can be designed and manufactured using the mentioned independency with the wide-band complete polarization conversion in the transmission and semi-reflection band-pass EM filter in some microwave frequency region.

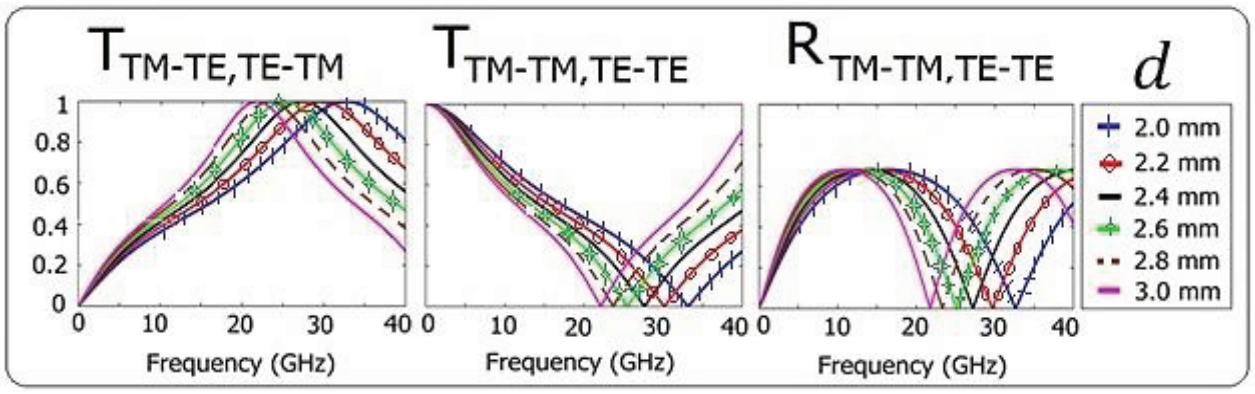

Fig. 4. Cross- and co-polarized transmission; and co-polarized reflection coefficients versus frequency with respect to the variation of the slab thickness.

D. Effect of the incident angle on the reflection and transmission

The last parameter to be investigated is the incident angle of the EM wave. The incident and the transmitted media are assumed to be free-space and CS has the following medium parameters: $d =$

$0.3mm$, $\xi_c = 0.003$, $\mu_c = \mu_0$, and $\varepsilon_c = 3\varepsilon_0$. The results are shown in Fig. 5 and Fig. 6. Symmetric and asymmetric quasi-reflection band-pass for the reflected wave occurs for both polarizations when the angle of incidence is varied. The symmetry of the reflection is degraded with the increase of the incident angle. Polarization conversion still occurs for both polarization for the studied incident angles, but the level of the cross-polarized transmission peak strongly depends on the angle of incidence. For TE incidence case, this peak level is high compared to TM incidence case. The structure is more sensitive to the variation of the incident angle for TM incidence situation. This means that while an unstable polarization conversion with respect to the peak level occurs for TM incident wave, a significant (including complete) polarization conversion occurs for TE incident wave. As a result, complete polarization conversion for TM incident case can be achieved for only small incident angles. Therefore, the incident angle plays an important role for the polarization conversion using the proposed system and one should take care of the incident angle in the design and optimization processes before the fabrication.

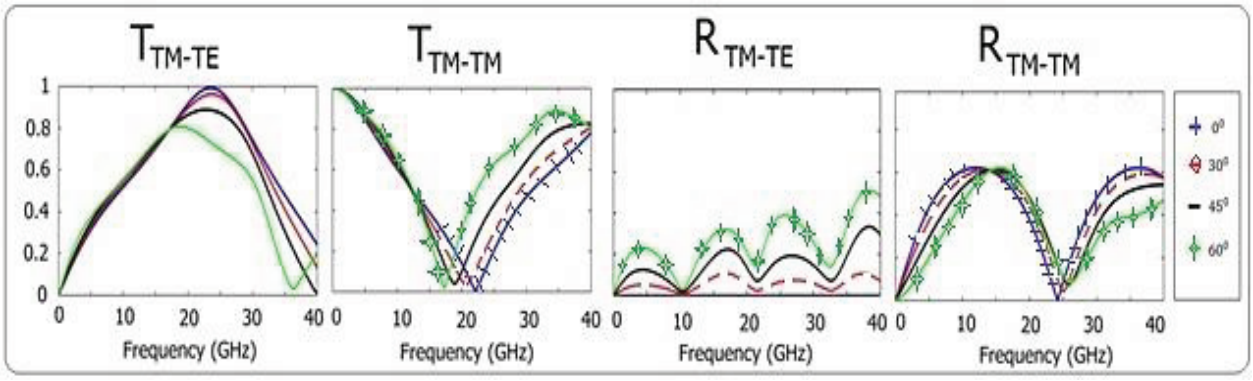

Fig. 5. Cross- and co-polarized transmission and reflection coefficients versus frequency with respect to the incident angle variation under TM incident wave.

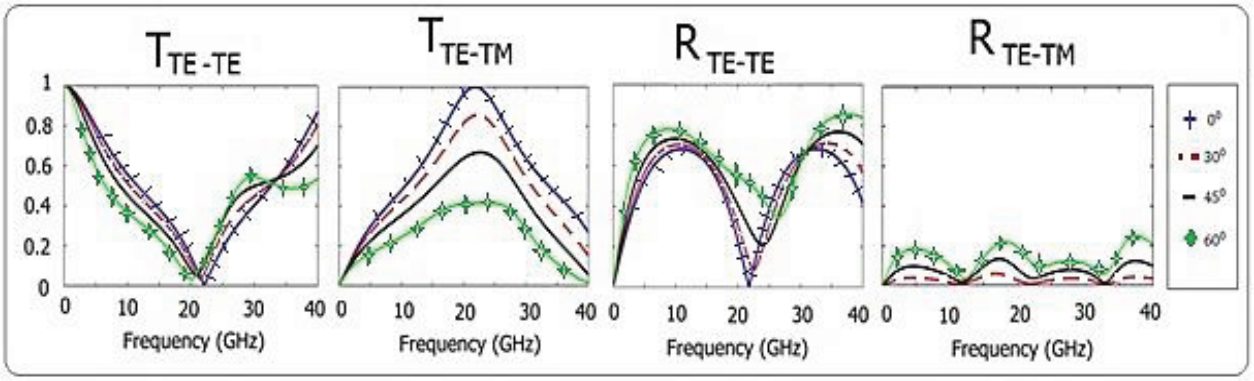

Fig. 6. Cross- and co-polarized transmission and reflection coefficients versus frequency with respect to the incident angle variation under TE incident wave.

IV. DESIGN AND OPTIMIZATION OF CHIRAL METAMATERIAL BASED ON SPLIT RECTANGULAR RESONATOR

In this part, the proposed structure given in the first section will be realized using full wave EM simulation software based on finite integration technique. The chirality parameter will be obtained and optimized to achieve a complete polarization conversion with wide-band transmission peak and antireflection property. The designed CMTM structure and its unit cell is shown in Fig. 7. The CMTM structure is formed by the periodic

arrangement of the unit cell based on split-rectangular-resonator (SRR). Commercial full wave EM simulation software is used in the simulation. FR4 is used as a substrate with the relative permittivity of 4.4, loss tangent of 0.002, and thickness of 0.28 mm. Copper is used for the metallic pattern with the conductivity of $5.8 \times 10^7\ S/m$ and thickness of 0.035 mm.

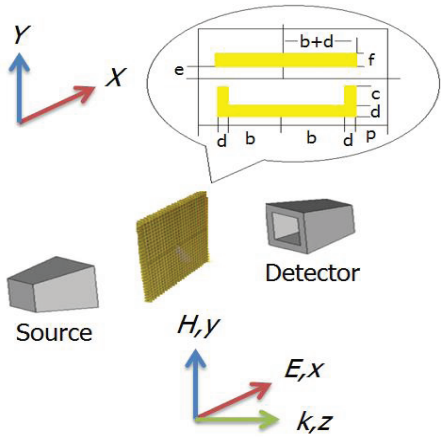

Fig. 7. Periodically arranged CMTM and its unit cell.

The optimized SRR dimensions are obtained using Interpolated Quasi Newton Approach in the simulation by setting them as parametric values. The augmentations can be realized by two different methods [26]; back tracking line-search and model-trust region methods. In the former method, step length is chosen to get satisfactory step, whereas a step is adjusted to reduce the norm of the local linear model in the latter method. Accuracy and S-parameter error threshold values are chosen as 10^{-6} and 0.01, respectively. The optimized dimensions are evaluated for different variables to provide polarization conversion and/or antireflection related to the results presented in the previous section. The computed optimized values are shown in Table 1 to Table 4. Table 1 shows the SRR dimensions when the chirality is changing which is related with the data of Section 3.1 (and Fig. 2). For example, there is a polarization conversion and antireflection phenomenon at the resonance frequency of 20.4 GHz when $\xi_c = 0.003$. The corresponding dimensions for SRR are given in Table 1 for the realization. Additionally, this is a kind of verification for the spectral location of the cross-polarized transmission peak and polarization rotation.

Table 1: The optimized SRR dimensions when the chirality is changing (related to Fig. 2)

ξ	f(GHz)	b(mm)	c(mm)	d(mm)	e(mm)	f(mm)	p(mm)
0.002	25.1	0.538	0.733	0.069	0.081	0.073	0.285
0.0025	23.3	1.962	0.733	0.054	0.196	0.050	0.977
0.003	22.1	0.538	1.967	0.196	0.192	0.196	0.977
0.0035	20.4	1.23	0.900	0.111	0.084	0.061	0.215
0.004	19.1	0.538	0.733	0.050	0.0538	0.053	0.123

Table 2 shows the SRR dimensions when the permittivity of CS is changing which is related with the data of Section 3.2 (and Fig. 3). For each design, there is a polarization rotation and antireflection property. Note that, the results of the table and corresponding data of Section 3.2 are in good agreement with each other.

Table 2: The optimized SRR dimensions when the permittivity of CS is changing (related to Fig. 3)

ε	f(GHz)	b(mm)	c(mm)	d(mm)	e(mm)	f(mm)	p(mm)
2	24.7	0.538	0.733	0.054	0.058	0.054	0.123
3	23.5	0.538	1.967	0.192	0.196	0.054	0.977
4	21.8	1.269	1.333	0.123	0.123	0.127	0.123
5	20.3	0.538	1.966	0.200	0.1962	0.054	0.123
6	19.0	1.1538	0.733	0.196	0.0538	0.0538	0.977

Table 3 and Table 4 show the SRR dimensions for the variation of thickness of CS and incident angle which are related with the data of Section 3.3 (Fig. 4) and Section 3.4 (Fig. 5). Once again, there is a polarization rotation and antireflection property for each design parameters. Note again, the results of the tables and corresponding data of Section 3 are in good agreement with each other.

Table 3: The optimized SRR dimensions when the thickness of CS is changing (related to Fig. 4)

d(mm)	f(GHz)	b(mm)	c(mm)	d(mm)	e(mm)	f(mm)	p(mm)
2	32.7	1.985	0.713	0.198	0.200	0.199	0.990
2.2	29.8	0.515	0.726	0.198	0.052	0.198	0.109
2.4	27.3	1.984	1.985	0.043	0.297	0.295	0.101
2.6	25.2	0.515	0.713	0.124	0.126	0.0515	0.545
2.8	23.4	1.985	1.514	0.237	0.277	0.123	1.156
3	21.8	0.416	0.515	0.043	0.045	0.043	0.101

Table 4: The optimized SRR dimensions when the incident angle is changing (related to Fig. 5)

θ(in °)	f(GHz)	b(mm)	c(mm)	d(mm)	e(mm)	f(mm)	p(mm)
0°	23.4	0.426	0.624	0.043	0.042	0.043	0.104
30°	23.7	0.228	0.426	0.033	0.3	0.115	1.486
45°	22.7	0.228	0.327	0.040	0.794	0.843	1.226
60°	18.8	0.228	0.327	0.040	0.03	0.099	1.486

V. VALIDATION OF THE NUMERICAL AND SIMULATION RESULTS

As a last investigation, the numerical (related to Section 3) and simulation (related to Section 4) results are calculated and compared. In the numerical computation, the thickness, dielectric constant, and chirality of CS is $d = 0{,}28\ mm$, $\varepsilon_c = 4\varepsilon_0$, and $\xi_c = 0.003$, in order. In the simulation, FR4 and copper are used for the substrate and metallic pattern, respectively, as mentioned in the previous section. The unit cell has the following dimensions: $b = 1.985\ mm$, $c = 1.514\ mm$, $d = 0.237\ mm$, $e = 0.277\ mm$, $f = 0.123\ mm$, and $p = 1.155\ mm$. The results are shown in Fig. 8. As seen, polarization rotation and antireflection phenomenon are noticed. Complete polarization rotation are observed around 23 GHz. The numerical and simulation results are in good agreement. Consequently, the theory is validated by numerical and simulation results. Therefore, one can realize a microwave polarization rotator or antireflection filter using the proposed model.

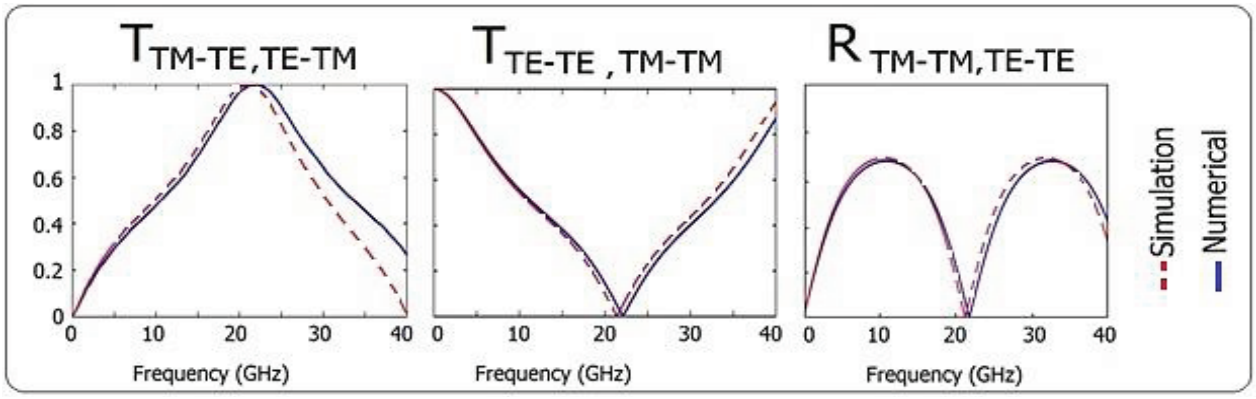

Fig. 8. Simulation and numerical results of CS and SRR based CMTM slab.

VI. CONCLUSION

The frequency response of CS is presented by theoretically and numerically. Then, a particular case is also studied by simulation, which means that the proposed CS is realized using full wave simulation software. The optical activity, EM filtering, and polarization rotation features of the structures with optimized parameters for the wide frequency region are presented via numerical and simulation results. The effects of the chirality, dielectric constant of CS, slab thickness, and incident angle are also investigated both for TE and TM cases. Complete polarization conversion and EM filtering are observed from the results of the parametric study. The mentioned properties are acquired using small chirality values. As known, new generation CMTMs existing in literature provide large/giant chirality values. Opposite to the existing studies, the proposed model (a kind of new generation CMTM) with small chirality shows optimum results within the wide frequency range. Additionally, this small chirality is sufficient for polarization rotation and EM filtering. According to the best of our knowledge, this kind of study (new generation CMTM with small chirality as a single slab and its application to the polarization conversion) is not studied in literature up to date. Consequently, the proposed structure can be utilized for EM filtering, and especially polarization conversion devices for wide range of microwave frequencies. As a result, this study paves the way towards the realization and fabrication of a polarization rotator and can be used for data transmission or sensing purposes.

REFERENCES

[1] A. Sihvola, "*Electromagnetic Emergence in Metamaterials*," Advances in Electromagnetics

of Complex Media and Metamaterials, S. Zouhdi, A. Sihvola, and M. Arsalane (eds.), vol. 89, NATO Science Series II: Mathematics, Physics, and Chemistry, Kluwer Academic, 2003.

[2] N. Engheta and R. W. Ziolkowski, *Metamaterials: Physics and Engineering Explorations*, Wiley-IEEE Press, Piscataway, NJ, 2006.

[3] L. Solymar and E. Shamonina, *Waves in Metamaterials*, Oxford University Press, New York, 2009.

[4] C. Sabah and S. Uckun, "Multilayer system of lorentz/drude type metamaterials with dielectric slabs and its application to electromagnetic filters," *Progress In Electromagnetics Research*, vol. 91, pp. 349-364, 2009.

[5] C. Sabah, H. T. Tastan, F. Dincer, K. Delihacioglu, M. Karaaslan, and E. Unal, "Transmission tunneling through the multi-layer double-negative and double-positive slabs," *Progress In Electromagnetics Research*, vol. 138, pp. 293-306, 2013.

[6] D. Jaggard, L. N. Engheta, M. W. Kowarz, P. Pelet, J. C. Liu, and Y. Kim, "Periodic chiral structures," *IEEE T. Antenn. Propag*., vol. 37, pp. 1447-1452, 1989.

[7] J. Lekner, "Optical properties of isotropic chiral media," *Pure Appl. Opt*., vol. 5, pp. 417-443, 1996.

[8] C. Sabah and S. Uckun, "Mirrors with chiral slabs," *J. Optoelectronics and Advanced Materials*, vol. 8, pp. 1918-1924, 2006.

[9] C. Sabah and H. G. Roskos, "Design of a terahertz polarization rotator based on a periodic sequence of chiral – metamaterial and dielectric slabs," *Progress In Electromagnetics Research*, vol. 124, pp. 301-317, 2012.

[10] J. Zhou, J. Dong, B. Wang, T. Koschny, M. Kafesaki, and C. M. Soukoulis, "Negative refractive index due to chirality," *Phys. Rev. B*, vol. 79, pp. 121104-4, 2009.

[11] W. Padilla, A. J. Taylor, C. Highstrete, M. Lee, and R. D. Averitt, "Dynamical electric and magnetic metamaterial response at terahertz frequencies," *Phys. Rev. Lett*., vol. 96, pp. 107401-4, 2006.

[12] Z. Li, R. Zhao, T. Koschny, M. Kafesaki, K. Alici, E. Colak, H. Caglayan, E. Ozbay, and C. M. Soukoulis, "Chiral metamaterials with negative refractive index based on four "U" split ring resonators," *Appl. Phys. Lett*., vol. 97, pp. 081901-3, 2010.

[13] R. Zhao, L. Zhang, J. Zhou, T. Koschny, and C. M. Soukoulis, "Conjugated gammadion chiral metamaterial with uniaxial optical activity and negative refractive index," *Phys. Rev. B*, vol. 83, pp. 035105-4, 2011.

[14] R. Zhao, T. Koschny, and C. M. Soukoulis, "Chiral metamaterials: retrieval of the effective parameters with and without substrate," *Opt. Express*, vol. 18, pp. 14553-67, 2010.

[15] U. C. Hasar, J. J. Barroso, M. Ertugrul, C. Sabah, and B. Cavusoglu, "Application of a useful uncertainty analysis as a metric tool for assessing the performance of electromagnetic properties retrieval methods of bianisotropic metamaterials," *Progress In Electromagnetics Research*, vol. 128, pp. 365-80, 2012.

[16] D. Jaggard, L. N. Engheta, M. W. Kowarz, P. Pelet, J. C. Liu, and Y. Kim, "Periodic chiral structures," *IEEE T. Antenn. Propag*., vol. 37, pp. 1447-1452, 1989.

[17] C. Zhangand and T. J. Cui, "Negative reflections of electromagnetic waves in a strong chiral medium," *Appl. Phys. Lett*., vol. 91, pp. 194101, 2007.

[18] J. C. Bose, "On the rotation of plane of polarization of electric waves by a twisted structure," *J. Proceedings of the Royal Society of London*, vol. 63, pp. 146-152, 1898.

[19] I. Tinoco and M. P. Freeman, "The optical activity of oriented copper helices, I. experimental," *J. Phys. Chem.*, vol. 61, pp. 1196-1200, 1957.

[20] C. Guerin, "Energy dissipation and absorption in resiprocal bi-isotropic media described by different formalism," *Progress In Electromagnetics Research*, vol. 9, pp. 31-44, 1994.

[21] F. Dincer, C. Sabah, M. Karaaslan, E. Unal, M. Bakir, and U. Erdiven, "Asymmetric transmission of linearly polarized waves and dynamically wave rotation using chiral metamaterial," *Progress In Electromagnetics Research*, vol. 140, pp. 227-239, 2013.

[22] Y. Cheng, Y. Nie, L. Wu, and R. Gong, "Giant circular dichroism and negative refractive index of chiral metamaterial based on split-ring resonators," *Progress In Electromagnetics Research*, vol. 138, pp. 421-432, 2013.

[23]S. J. Orfanidis, *Electromagnetic Waves and Antennas*, online text book, Rutgers University, 2004 (ece.rutgers.edu/~orfanidi/ewa/).
[24]D. L. Jaggard, A. R. Mickelson, and C. H. Papas, "On electromagnetic waves in chiral media," *Appl. Physics*, vol. 18, pp. 211-216, 1979.
[25]N. Engheta and D. L. Jaggard, "Electromagnetic chirality and its applications," *IEEE AP-S Newsletter*, vol. 30, pp. 6-12, 1988.
[26]J. E. Dennis and J. J. More, "Quasi-Newton methods, motivation and theory," *SIAM Review*, vol. 19, pp. 46-89, 1977.

Ibrahim Comez received the M.S. degree in Physics Department from the University of Cukurova, Adana, Turkey. He is currently studying Metamaterials and Chiral Media as a Ph.D. student. His research interests are metamaterials, solid state physics, cihral, and anisotropic media.

Muharrem Karaaslan received the Ph.D. degree in Physics Department from the University of Cukurova, Adana, Turkey, in 2009. He is the co-author of about 20 scientific contributions published in journals and conference proceedings. His research interest are applications of metamaterials, analysis and synthesis of antennas, and waveguides.

Furkan Dincer received the B.Sc., M.Sc., and Ph.D. degrees in Electrical and Electronics Engineering from Sutcu Imam, Yuzuncu Yil and Mustafa Kemal Universities, Turkey. His research interests are related with the functional microwave structures and metamaterials.

Faruk Karadag received the Ph.D. degree in Physics Department from the University of Çukurova, Adana, Turkey, in 2002. He is the co-author of about 25 scientific contributions published in international journals and conference proceedings. His research interest includes the applications of metamaterials, solid state physics, and anisotropic media.

Cumali Sabah received the B.Sc., M.Sc., and Ph.D. degrees in Electrical and Electronics Engineering from the University of Gaziantep, Turkey. He is currently with Middle East Technical University ─ Northern Cyprus Campus. His research interests include the microwave and electromagnetic investigation of unconventional materials and structures, wave propagation, scattering, complex media, metamaterials and their applications.